

RESEARCH ARTICLE

Differences in Transport Mechanisms of *trans*-1-Amino-3- ^{18}F Fluorocyclobutanecarboxylic Acid in Inflammation, Prostate Cancer, and Glioma Cells: Comparison with L-[Methyl- ^{11}C]Methionine and 2-Deoxy-2- ^{18}F Fluoro-D-Glucose

Shuntaro Oka,^{1,5} Hiroyuki Okudaira,¹ Masahiro Ono,^{1,2} David M. Schuster,³ Mark M. Goodman,³ Keiichi Kawai,^{2,4} Yoshifumi Shirakami¹

¹Research Center, Nihon Medi-Physics Co., Ltd, Chiba, Japan

²Graduate School of Medical Science, Kanazawa University, Ishikawa, Japan

³Division of Nuclear Medicine and Molecular Imaging, Department of Radiology and Imaging Sciences, Emory University, Atlanta, GA, USA

⁴Biomedical Imaging Research Center, University of Fukui, Fukui, Japan

⁵Kitasode 3-1, Sodegaura, Chiba, 299-0266, Japan

Abstract

Purpose: We aimed to elucidate *trans*-1-amino-3- ^{18}F fluorocyclobutanecarboxylic acid (*anti*- ^{18}F FACBC) uptake mechanisms in inflammatory and tumor cells, in comparison with those of L-[methyl- ^{11}C]methionine (^{11}C Met) and 2-deoxy-2- ^{18}F fluoro-D-glucose (^{18}F FDG).

Procedures: Using carbon-14-labeled tracers, *in vitro* time-course, pH dependence, and competitive inhibition uptake experiments were performed in rat inflammatory (T cells, B cells, granulocytes, macrophages), prostate cancer (MLLB2), and glioma (C6) cells.

Results: *Anti*- ^{14}C FACBC uptake ratios of T/B cells to tumor cells were comparable, while those of granulocytes/macrophages to tumor cells were lower than those for ^{14}C FDG. Over half of *anti*- ^{14}C FACBC uptake by T/B and tumor cells was mediated by Na^+ -dependent amino acid transporters (system ASC), whereas most ^{14}C Met transport in all cells was mediated by Na^+ -independent carriers (system L).

Conclusions: The low *anti*- ^{18}F FACBC accumulation in granulocytes/macrophages may be advantageous in discriminating inflamed regions from tumors. The significant *anti*- ^{18}F FACBC uptake in T/B cells may cause false-positives in some cancer patients who undergo FACBC-positron emission tomography (PET).

Key words: *Anti*- ^{18}F FACBC, *Anti*- ^{14}C FACBC, ^{11}C Met, ^{14}C Met, ^{18}F FDG, ^{14}C FDG, Amino acid transporters, Inflammatory cells, Prostate cancer, Glioma

Electronic supplementary material The online version of this article (doi:10.1007/s11307-013-0693-0) contains supplementary material, which is available to authorized users.

Correspondence to: Shuntaro Oka; e-mail: shuntaro_oka@nmp.co.jp

Introduction

2-Deoxy-2- ^{18}F fluoro-D-glucose (^{18}F FDG) is the most frequently used positron emission tomog-

raphy (PET) tracer for cancer imaging; however, it accumulates in inflammatory regions, potentially resulting in false-positive uptake [1]. Alternatively, L-[methyl- ^{11}C]methionine (^{11}C Met), an amino acid (AA) PET tracer, is useful for tumor imaging and monitoring of therapeutic effects, especially in brain, due to its low physiological accumulation in normal cerebral tissue and inflamed lesions [2]. However, its use is restricted to facilities with a cyclotron, because carbon-11 has a short half-life (20 min). To overcome this, several synthetic fluorine-18-labeled AA PET tracers (half-life: 110 min) such as *trans*-1-amino-3- ^{18}F fluorocyclobutanecarboxylic acid (*anti*- ^{18}F FACBC) have been developed [3]. We and others have reported that the imaging potential of *anti*- ^{18}F FACBC for glioma and prostate cancer (PCa) is comparable to that of ^{18}F FDG and ^{11}C Met in preclinical and clinical studies [3–6]. Moreover, we previously reported that *anti*- ^{18}F FACBC accumulation was higher in subcutaneous PCa than in lymphadenitis in an animal model [5]. However, a recent clinical study showed no separation between malignant and non-malignant sextants by standardized uptake value (SUV) on FACBC-PET in some PCa patients [7]. We speculated that the relatively high SUV in non-malignant sextants might be explained by *anti*- ^{18}F FACBC uptake and accumulation in inflammatory cells, because PCa usually contains inflamed tissue [8].

Transport of *anti*- ^{18}F FACBC into cells is mediated by AA transporter(s) (AAT(s)) [9–11], which are either Na^+ -dependent or Na^+ -independent, based on the sodium ion requirement for transport [12]. AATs are further categorized into "systems" (e.g., system A, ASC, L) based on their substrate selectivity [12]. Moreover, extracellular pH affects AAT activity [12]. We previously reported that the main AATs mediating *trans*-1-amino-3-fluoro[1- ^{14}C]cyclobutanecarboxylic acid (*anti*- ^{14}C FACBC) uptake in human PCa cell lines were Na^+ -dependent system ASC (especially ASCT2) and Na^+ -independent system L (especially LAT1), and the contribution of system L was enhanced in acidic pH as is present in an intratumoral environment [9–11].

Although *anti*- ^{18}F FACBC transport mechanisms in cancer cells have been demonstrated, transport in inflammatory cells remains unclear. Therefore, we compared *anti*- ^{18}F FACBC uptake in rat inflammatory cells (T cells, B cells, granulocytes, macrophages) with that in rat PCa (MLLB2) and glioma (C6) cell lines, and also to that of ^{18}F FDG and ^{11}C Met.

Materials and Methods

Chemicals

All reagents were purchased from Life Technologies (Carlsbad, CA, USA), Sigma-Aldrich (St. Louis, MO, USA), Nacalai Tesque (Kyoto, Japan), and Wako (Osaka, Japan), unless otherwise stated. In all experiments, carbon-14-labeled compounds were used as tracers. *Anti*- ^{14}C FACBC was synthesized by Sekisui Medical (Tokyo, Japan) as described previously [10], with specific activity and radiochemical purity of 2.08 GBq/mmol and >98.0 %, respectively. L-[Methyl- ^{14}C]methionine (^{14}C MET) and 2-fluoro-2-deoxy-D-glucose, [^{14}C (U)] (^{14}C FDG) were purchased from

American Radiolabeled Chemicals (St. Louis, MO, USA), with specific activities of 2.04 and 11.10 GBq/mmol, respectively.

Animals and Cells

All animal handling and experimentation procedures accorded with protocols approved by the committee on animal welfare at Nihon Medi-Physics. Male Copenhagen rats (CLEA, Tokyo, Japan) were used in experiments at 11–16 weeks of age. In all animal preparations, animals were anesthetized with 1 % isoflurane (Mylan, Pittsburgh, PA, USA).

Inflammatory cells were isolated from Copenhagen rats using standard methods based on density gradient centrifugation (T cells, B cells, and granulocytes) and adhesion-mediated purification on culture dishes (macrophages). T cells and granulocytes were stimulated with concanavalin A (0.25 $\mu\text{g}/\text{ml}$) and phorbol 12-myristate 13-acetate (100 nM), respectively; B cells and macrophages were stimulated with lipopolysaccharide (5 $\mu\text{g}/\text{ml}$) from *Escherichia coli* O55:B5. See Supplemental Information for details.

Rat PCa (MLLB2) and glioma (C6) cell lines were obtained from American Type Culture Collection (ATCC, Manassas, VA, USA), and maintained in RPMI1640 and modified Eagle medium, respectively, supplemented with 10 % fetal bovine serum (ATCC), 100 $\mu\text{g}/\text{ml}$ streptomycin, 100 U/ml penicillin, and 2 mM L-glutamine.

Time-Course Tracer Uptake Experiments

Time-course tracer uptake experiments were carried out based on previous studies [5, 10] using 10 μM *anti*- ^{14}C FACBC, ^{14}C Met, and ^{14}C FDG. In these experiments, we used glucose-free Hanks' balanced salt solution containing Mg^{2+} and Ca^{2+} (HBSS(+)) because D-glucose inhibits ^{14}C FDG uptake. Briefly, T/B cells (5.0×10^5) or granulocytes (2.5×10^5) were suspended in 100 μl glucose-free HBSS(+) including tracers, and placed in 96-well culture plates. For macrophages, 150 μl of glucose-free HBSS(+) containing tracers was added to macrophages cultivated in 48-well culture plates (3.0×10^5 /well). MLLB2 (5.0×10^4 /well) and C6 (1.0×10^5 /well) cells were seeded in 24-well culture plates, and media were replaced with 300 μl glucose-free HBSS(+) containing tracers on day 2 of cultivation. Cells were incubated for 5, 15, 30, and 60 min at 37 $^\circ\text{C}$, washed with ice-cold glucose-free HBSS(+), and lysed in 0.1 N NaOH. Radioactivity in cell lysates was measured with a Tri-Carb 2910TR liquid scintillation counter (Perkin Elmer, Waltham, MA, USA). Protein concentrations of cell lysates were determined using the BCA Protein Assay Kit (Thermo Fisher Scientific, Waltham, MA, USA). Tracer uptake was expressed as $\mu\text{mol}/\text{mg}$ protein.

pH-Dependent Tracer Uptake Experiments

Anti- ^{14}C FACBC and ^{14}C Met uptake experiments were conducted using activated T/B cells and tumor cells according to the procedure described above. Three types of uptake buffer, sodium, choline, and lithium, were used, because 1) all AATs function in sodium buffer, 2) only Na^+ -independent AATs function in choline buffer, and 3) all Na^+ -independent AATs and the Na^+ -dependent N and y⁺L AAT systems function in lithium buffer [12, 13]. The sodium buffer contained 140 mM NaCl, 5 mM KCl, 5.6 mM D-glucose, 0.9 mM CaCl_2 ,

1.0 mM MgCl₂, 0.3 mM Na₂HPO₄, and 0.4 mM KH₂PO₄; pH was adjusted with 4-morpholineethanesulfonic acid to pH 6.0 and with 4-(2-hydroxyethyl)piperazine-1-ethanesulfonic acid (HEPES) to pH 7.0 and 8.0. The choline buffer contained 140 mM choline chloride and 0.3 mM K₂HPO₄ instead of sodium chloride and Na₂HPO₄. The lithium buffer contained lithium chloride instead of choline chloride. Tracer uptake times were 5 min for MLLB2 and C6 and 10 min for T/B cells, because *anti*-[¹⁴C]FACBC uptake in each cell type was linear up to these time-points (data not shown). Termination of tracer uptake, cell washing, and radioactivity and cellular protein measurements were conducted as described above. Tracer uptake was expressed as pmol/mg protein/min. The contributions of Na⁺-dependent and Na⁺-independent transport systems to *anti*-[¹⁴C]FACBC and [¹⁴C]Met uptake were estimated using the following formulas:

$$\begin{aligned} \text{Na}^+ \text{-independent AATs} &= V_C \\ \text{Na}^+ \text{-dependent AATs} &= V_S - V_C \\ \text{system N and } y^+ \text{L AATs} &= V_L - V_C \\ \text{Na}^+ \text{-dependent AATs except for system N and } y^+ \text{L AATs} &= V_S - V_L, \end{aligned}$$

where V_S , V_C , and V_L are the amounts of tracer uptake in sodium, choline, and lithium buffers, respectively. The transport of tracers in sodium buffer at each pH was normalized to 100%. If tracer uptake in choline buffer was higher than that in sodium buffer at each pH, the contribution of Na⁺-dependent AATs was taken as zero. If tracer uptake in lithium buffer was higher than that in sodium buffer at each pH, the uptake in lithium buffer was considered the same as in sodium buffer.

Competitive Inhibition Tracer Uptake Experiments

Sodium, choline, and lithium buffers, adjusted to pH 7.2–7.3 with HEPES, were used. Uptake experiments were performed as described above in the presence of 2 mM naturally occurring or synthetic AAs as inhibitors. The synthetic AAs and their AAT specificities are (summarized in Table S1): 2-amino-bicyclo[2,2,1]heptane-2-carboxylic acid (BCH), systems L, B⁰, and B⁰⁺; *N*-ethylmaleimide (NEM), systems L (except LAT1), b⁰⁺, and y⁺; and 2-(methylamino)-isobutyric acid (MeAIB), systems A, IMINO, and PAT. Naturally occurring AAs are not AAT-specific, but some show preference for certain AATs; thus, we used some naturally occurring AAs (L-forms) as inhibitors, as follows (preferred AATs in parentheses): glutamine, systems A, ASC (ASCT2), B⁰ (B⁰AT1), N, y⁺L, L (LAT2), and B⁰⁺; serine, systems A, ASC, B⁰ (B⁰AT1), N (SNAT5), L (LAT2), asc, and B⁰⁺; phenylalanine, systems B⁰, y⁺L, L, T, B⁰⁺, and b⁰⁺; proline, system A (ATA2), ASC (ASCT1), G-like, B⁰, IMINO, B⁰⁺, and PAT; glycine, systems A (except for ATA1), B⁰ (B⁰AT1), N (SNAT5), y⁺L, L (LAT2), asc, B⁰⁺, and PAT; glutamate, systems y⁺L, X_{A,G}, and X_C⁻; arginine, systems B⁰⁺, b⁰⁺, y⁺L, and y⁺. *Anti*-[¹⁴C]FACBC and [¹⁴C]Met transport (control) in the absence of inhibitors in each buffer was normalized to 100%, and the inhibitory effects of naturally occurring and synthetic AAs on the uptake of both tracers were calculated as a percentage of control. To simplify the results, the intensity of the inhibitory effects was categorized into five classes based on average inhibitory rates: ≤19.9%, 20.0–39.9%, 40.0–59.9%, 60.0–79.9%, and ≥80.0%.

Statistics

Experiments were repeated at least twice. All results are expressed as mean±SD unless otherwise stated. All statistical analyses were performed using SAS for Windows (Ver. 5, SAS Institute, Cary, NC, USA). For datasets with normal distribution, homogeneity of variance was analyzed by the *F*-test; homogeneous data were analyzed using the two-tailed unpaired Student's *t*-test, whereas non-homogeneous data were analyzed using the Welch *t*-test. The Wilcoxon rank sum test was used for non-normal datasets. $P < 0.05$ was considered significant.

Results

Time-Course Tracer Uptake Experiments

The time-course of *anti*-[¹⁴C]FACBC, [¹⁴C]Met, and [¹⁴C]FDG uptake was determined in inflammatory cells and tumor cells (Fig. 1); thereafter, uptake ratios of activated inflammatory cells to non-stimulated (NS) inflammatory cells and of activated inflammatory cells to tumor cells were calculated from the results in Fig. 1 (Table 1). Although *anti*-[¹⁴C]FACBC uptake in all cells except granulocytes tended to plateau at 15 or 30 min of incubation, [¹⁴C]Met and [¹⁴C]FDG uptake increased with time (Fig. 1). [¹⁴C]FDG uptake by activated inflammatory cells and tumor cells was significantly higher than those of AA tracers (Fig. 1, note difference in *Y*-axis scale between tracers). Upon inflammatory cell activation, *anti*-[¹⁴C]FACBC uptake tended to be accelerated except in macrophages (Fig. 1a,b, Table 1), whereas [¹⁴C]Met uptake was increased in T/B cells, but not in granulocytes/macrophages (Fig. 1c,d, Table 1). All activated cells took up more [¹⁴C]FDG than did non-stimulated cells (Fig. 1e,f, Table 1).

Anti-[¹⁴C]FACBC uptake was similar in activated T/B cells and MLLB2/C6 cells, but clearly lower in activated granulocytes/macrophages (Fig. 1a,b). [¹⁴C]Met uptake in activated T cells and [¹⁴C]FDG uptake in all activated cells except B cells were similar to that in tumor cells (Fig. 1c–f). Uptake ratios of activated inflammatory cells to tumor cells show the relatively high uptake of *anti*-[¹⁴C]FACBC in activated T/B cells (Table 1).

pH-Dependent Tracer Uptake Experiments

The transport activities of some AATs are affected by extracellular pH changes. Some examples of such pH-dependent activity changes are given in Table S1. Thus, we investigated the influence of extracellular pH on *anti*-[¹⁴C]FACBC and [¹⁴C]Met uptake in activated T/B cells and tumor cells, which indicated relatively high AA tracer uptake.

[¹⁴C]Met uptake tended to be higher in acidic pH in all conditions (Fig. 2a–d). Although similar *anti*-[¹⁴C]FACBC uptake trends were observed in the absence of Na⁺, *anti*-[¹⁴C]FACBC uptake in sodium buffer was higher at neutral and acidic pH than at alkaline pH (Fig. 2a–d).

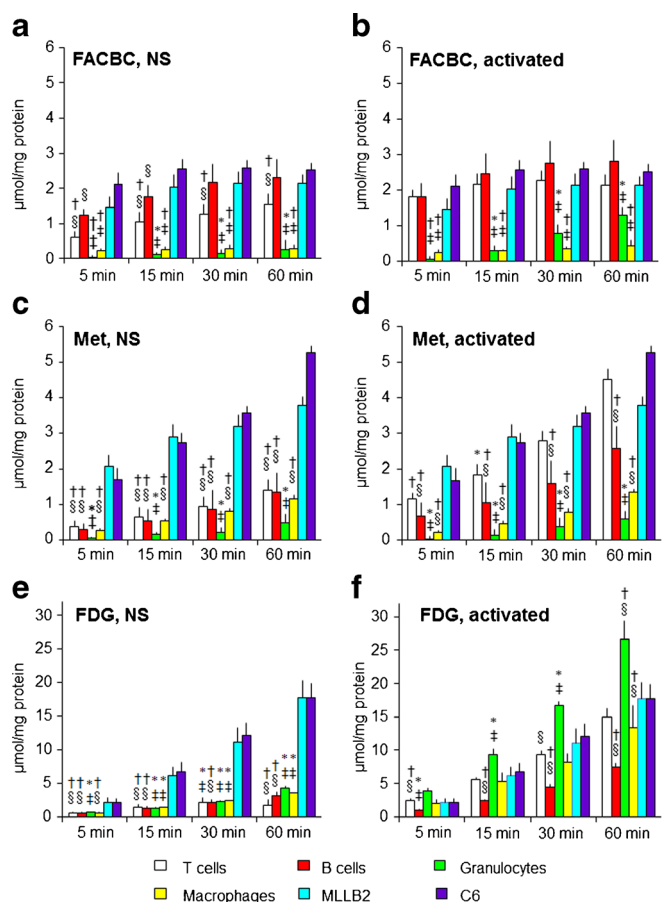


Fig. 1. Time-course of *anti*-[¹⁴C]FACBC (**a, b**), [¹⁴C]Met (**c, d**), and [¹⁴C]FDG (**e, f**) uptake in non-stimulated (NS) (**a, c, e**) and activated (**b, d, f**) rat T cells, B cells, granulocytes, macrophages, and rat-derived PCa (MLLB2) and glioma (C6) cell lines ($n=6-12$). Statistical analyses were conducted between each type of inflammatory cells and MLLB2 or C6. * $P < 0.05$ vs. MLLB2, † $P < 0.01$ vs. MLLB2, ‡ $P < 0.05$ vs. C6, § $P < 0.01$ vs. C6.

Na^+ -dependent *anti*-[¹⁴C]FACBC transport tended to be more active in neutral to alkaline pH, whereas Na^+ -independent transport tended to be more active in acidic pH (Fig. 2e-h). The contributions of Na^+ -dependent AATs except system N and y^{L} to *anti*-[¹⁴C]FACBC uptake in T/B cells were 70–90 %, while 50–100 % of [¹⁴C]Met transport was mediated in an Na^+ -independent manner (Fig. 2e,f). In tumor cells, although *anti*-[¹⁴C]FACBC transport was predominantly Na^+ -independent in acidic pH (60–70 %), the contribution of Na^+ -dependent uptake, except in system N and/or y^{L} , was enhanced up to 60 % at pH 8.0 (Fig. 2g,h). Almost all [¹⁴C]Met transport in tumor cells was Na^+ -independent. The contributions of system N and/or y^{L} to *anti*-[¹⁴C]FACBC and [¹⁴C]Met uptake were 10 % at most in T/B cells and tumor cells.

As described above, time-course experiments of *anti*-[¹⁴C]FACBC, [¹⁴C]Met, and [¹⁴C]FDG uptake were conducted in the absence of D-glucose to avoid [¹⁴C]FDG uptake inhibition by D-glucose. However, because D-glucose is an important fuel for cells, utilized at a high rate by inflammatory cells during activation and by cancer cells, uptake ratios of activated inflammatory cells to tumor cells in the presence of D-glucose were calculated from the data in Fig. 2a-d. *Anti*-[¹⁴C]FACBC and [¹⁴C]Met uptake ratios at pH 7.0 (Table 2), were lower than those in Table 1, indicating that although the inflammatory cell to tumor cell uptake ratios of *anti*-[¹⁴C]FACBC and [¹⁴C]Met are improved under physiological conditions, *anti*-[¹⁴C]FACBC ratios in activated T/B cells remain consistently higher than other ratios. Extracellular pH changes had little effect on these ratios.

Competitive Inhibition Tracer Uptake Experiments

To narrow down AATs involved in *anti*-[¹⁴C]FACBC and [¹⁴C]Met uptake, we investigated their uptake in the presence of naturally occurring/synthetic AAs (Fig. 3, Figs. S2–S5). In

Table 1. Uptake ratio of activated inflammatory cells to non-stimulated inflammatory cells, and of activated inflammatory cells to tumor cells (without D-glucose)

Activated inflammatory cells	Incubation time (min)	<i>Anti</i> -[¹⁴ C]FACBC			[¹⁴ C]Met			[¹⁴ C]FDG		
		vs. NS	vs. MLLB2	vs. C6	vs. NS	vs. MLLB2	vs. C6	vs. NS	vs. MLLB2	vs. C6
T cells	5	3.0	1.2	0.9	3.1	0.6	0.7	4.6	1.2	1.2
	15	2.1	1.1	0.8	2.9	0.6	0.7	4.1	0.9	0.8
	30	1.8	1.1	0.9	2.9	0.9	0.8	4.4	0.8	0.8
	60	1.4	1.0	0.8	3.2	1.2	0.9	9.2	0.8	0.8
B cells	5	1.5	1.2	0.9	2.3	0.3	0.4	2.0	0.5	0.5
	15	1.4	1.2	1.0	2.0	0.4	0.4	2.1	0.4	0.4
	30	1.3	1.3	1.1	1.8	0.5	0.4	2.2	0.4	0.4
	60	1.2	1.3	1.1	1.9	0.7	0.5	2.4	0.4	0.4
Granulocytes	5	1.5	0.04	0.02	1.1	0.02	0.02	6.2	1.9	1.9
	15	2.5	0.1	0.1	1.0	0.1	0.1	7.2	1.5	1.4
	30	5.4	0.4	0.3	1.7	0.1	0.1	7.2	1.5	1.4
	60	4.9	0.6	0.5	1.3	0.2	0.1	6.3	1.5	1.5
Macrophages	5	1.1	0.2	0.1	0.9	0.1	0.1	3.5	0.9	1.0
	15	1.1	0.1	0.1	0.9	0.2	0.2	3.9	0.9	0.8
	30	1.1	0.2	0.1	1.0	0.2	0.2	3.5	0.7	0.7
	60	1.5	0.2	0.2	1.2	0.4	0.3	3.9	0.8	0.8

These ratios were calculated from Fig. 1. NS: non-stimulated

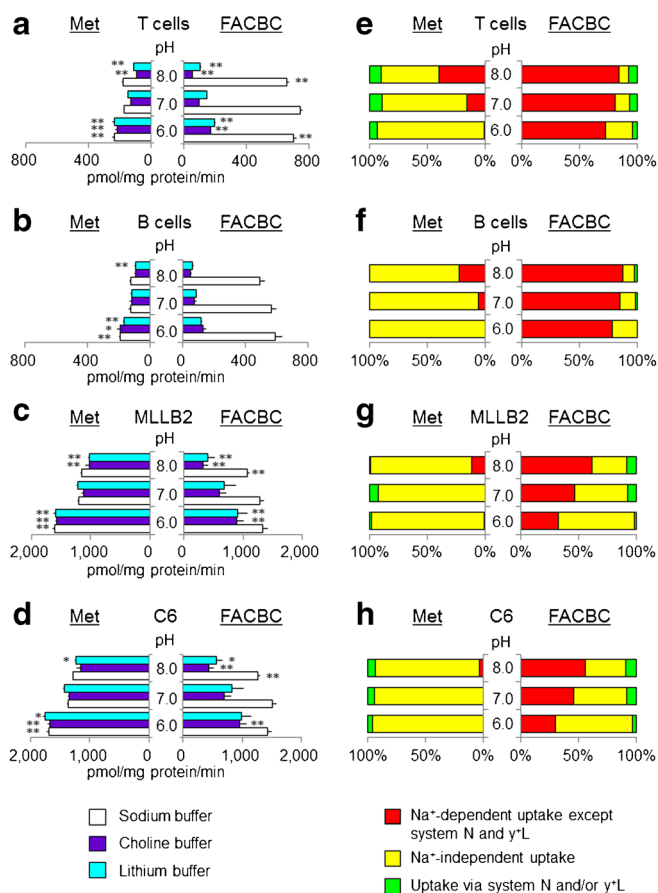


Fig. 2. pH-dependence of *anti*-[¹⁴C]FACBC and [¹⁴C]Met uptake, and contributions of Na⁺-dependent and Na⁺-independent transport systems to the uptake of AA tracers into rat activated T cells (**a, e**), B cells (**b, f**), and PCa (MLLB2) (**c, g**) and glioma (C6) (**d, h**) cell lines. **a–d** Cells were incubated with 10 μM *anti*-[¹⁴C]FACBC (FACBC) or [¹⁴C]Met (Met) in sodium, choline, or lithium buffer (*n*=6). **P*<0.05, ***P*<0.01 relative to *anti*-[¹⁴C]FACBC uptake values at pH 7.0 in sodium, choline, and lithium buffer. **e–h** Contributions of Na⁺-independent uptake, uptake via systems N and/or y⁺L, and Na⁺-dependent uptake except for systems N and y⁺L to *anti*-[¹⁴C]FACBC and [¹⁴C]Met uptake were calculated from the data in **a–d**.

sodium buffer, small neutral AAs such as glutamine and serine, which are preferentially transported by systems A, ASC, B⁰ (B⁰AT1), N, y⁺L, L (LAT2), asc, and/or B^{0,+}, inhibited ≥80 % *anti*-[¹⁴C]FACBC uptake by T/B cells. On the contrary,

inhibition by glutamate, arginine, and MeAIB, which are substrates for systems B^{0,+}, b^{0,+}, y⁺L, y⁺, X_{A,G}⁻, X_C⁻, A, IMINO, and/or PAT, was ≤19.9 %. These results suggest that systems ASC, B⁰, N, L, and/or asc are the important AATs that mediate *anti*-[¹⁴C]FACBC uptake in activated T/B cells. Inhibition by phenylalanine and BCH, substrates of systems B⁰, y⁺L, T, L, B^{0,+}, and/or b^{0,+}, on *anti*-[¹⁴C]FACBC transport by T/B cells was 20.0–59.9 % in the presence of Na⁺, but ≥80.0 % in choline buffer (Fig. 3a,b). Although glutamine in the lithium buffer showed ≥80.0 % inhibitory effect for *anti*-[¹⁴C]FACBC uptake in T/B cells (Fig. 3c), this does not imply *anti*-[¹⁴C]FACBC transport via system N AATs, because glutamine inhibited the transport ≥80.0 % even in choline buffer (Fig. 3b). These results indicate that system ASC is the main AAT among Na⁺-dependent AATs for *anti*-[¹⁴C]FACBC transport in T/B cells (Figs. 2e,f and 3). System L is also involved in Na⁺-independent *anti*-[¹⁴C]FACBC transport, although its contribution was 20 % at most (Fig. 2e,f).

System L is thought to be the main AAT for [¹⁴C]Met uptake in T/B cells, because most [¹⁴C]Met transport was mediated in an Na⁺-independent manner (Fig. 2e,f) and the representative substrates for system L such as phenylalanine and BCH showed strong inhibitory effects in choline buffer (Fig. 3b).

In neutral conditions, Na⁺-dependent and Na⁺-independent *anti*-[¹⁴C]FACBC transport had similar contributions in MLLB2 and C6 cells (Fig. 2g,h). *Anti*-[¹⁴C]FACBC inhibition by naturally occurring/synthetic AAs was also similar between both tumor cell lines (Fig. 3). In the presence of Na⁺, glutamine and serine showed the strongest inhibition of *anti*-[¹⁴C]FACBC uptake, followed by phenylalanine, proline, glycine, and BCH. Inhibitory rates by glutamate, arginine, NEM, and MeAIB were ≤19.9 %. Removal of Na⁺ from the buffer led to ≥80.0 % inhibition by phenylalanine and BCH as well as glutamine and serine. In lithium buffer, glutamine strongly inhibited *anti*-[¹⁴C]FACBC uptake in tumor cells as well as T/B cells, but this is not due to transport via system N as mentioned above. These results suggest that systems ASC and L are the main AATs in Na⁺-dependent and Na⁺-independent *anti*-[¹⁴C]FACBC transport, respectively.

System L is thought to be the main AAT for [¹⁴C]Met transport in MLLB2 and C6 cells, for the same reasons as mentioned above.

Table 2. Uptake ratio of activated inflammatory cells to tumor cells (with D-glucose)

Activated inflammatory cells	pH	<i>Anti</i> -[¹⁴ C]FACBC		[¹⁴ C]Met	
		vs. MLLB2	vs. C6	vs. MLLB2	vs. C6
T cells	6.0	0.5	0.5	0.1	0.1
	7.0	0.6	0.5	0.1	0.1
	8.0	0.6	0.5	0.2	0.1
B cells	6.0	0.4	0.4	0.1	0.1
	7.0	0.4	0.4	0.1	0.1
	8.0	0.5	0.4	0.1	0.1

These ratios were calculated from Fig. 2a–d

a Sodium buffer

Cells		T cells		B cells		MLLB2		C6	
Tracers		F	M	F	M	F	M	F	M
AAs	Gln	Red	Yellow	Red	Green	Red	Red	Red	Yellow
	Ser	Red	Green	Red	Cyan	Red	Yellow	Red	Yellow
	Phe	Cyan	Green	Cyan	Green	Green	Red	Cyan	Red
	Pro	Green	Grey	Green	Grey	Green	Grey	Green	Green
	Gly	Yellow	Cyan	Yellow	Grey	Green	Cyan	Green	Green
	Glu	Grey	Grey	Grey	Grey	Grey	Grey	Grey	Grey
	Arg	Grey	Grey	Grey	Grey	Grey	Grey	Grey	Cyan
	BCH	Green	Yellow	Green	Grey	Green	Red	Green	Red
	NEM	Yellow	Cyan	Yellow	Cyan	Grey	Grey	Grey	Grey
	MeAIB	Grey	Grey	Grey	Grey	Grey	Grey	Grey	Grey

b Choline buffer

Cells		T cells		B cells		MLLB2		C6	
Tracers		F	M	F	M	F	M	F	M
AAs	Gln	Red	Yellow	Red	Green	Red	Red	Yellow	Red
	Ser	Yellow	Green	Yellow	Cyan	Red	Red	Red	Yellow
	Phe	Red	Red	Red	Red	Red	Red	Red	Red
	Pro	Cyan	Grey	Grey	Grey	Grey	Grey	Grey	Grey
	Gly	Grey	Grey	Grey	Grey	Cyan	Grey	Green	Cyan
	Glu	Grey	Grey	Grey	Grey	Grey	Grey	Grey	Grey
	Arg	Grey	Grey	Grey	Grey	Grey	Grey	Cyan	Cyan
	BCH	Red	Yellow	Red	Yellow	Red	Red	Red	Red
	NEM	Cyan	Grey	Cyan	Cyan	Green	Grey	Cyan	Grey
	MeAIB	Grey	Grey	Grey	Grey	Grey	Grey	Grey	Grey

c Lithium buffer

Cells		T cells		B cells		MLLB2		C6	
Tracers		F	M	F	M	F	M	F	M
AAs	Gln	Red	Red	Red	Yellow	Red	Red	Red	Red
	Arg	Cyan	Green	Grey	Grey	Grey	Grey	Grey	Cyan

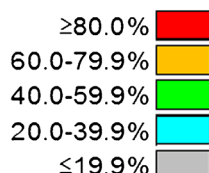


Fig. 3. Competitive inhibition of *anti*-¹⁴C]FACBC and [¹⁴C]Met transport in rat activated T cells and B cells, and PCa (MLLB2) and glioma (C6) cell lines in sodium (a), choline (b), and lithium (c) buffer ($n=5-21$). The intensity of the calculated inhibitory effect was categorized into five classes as indicated.

Discussion

Here, we compared the uptake of *anti*-¹⁴C]FACBC, [¹⁴C]Met, and [¹⁴C]FDG in rat inflammatory cells (T cells, B cells, granulocytes, macrophages) and tumor cell lines (MLLB2 and C6) by time-course experiments. We found that the uptake of tracers used in this study was enhanced with inflammatory cell activation, and relatively high inflammatory cell to tumor cell *anti*-¹⁴C]FACBC uptake ratios in T/B cells, comparable to or higher than those of [¹⁴C]FDG. Next, we elucidated differences in *anti*-¹⁴C]FACBC and [¹⁴C]Met transport mechanisms between

inflammatory and tumor cells through a series of pH dependency and competitive inhibition uptake experiments. We demonstrated that (1) Na⁺-dependent (especially system ASC) and Na⁺-independent (especially system L) AATs are likely the main route of *anti*-¹⁴C]FACBC and [¹⁴C]Met uptake, respectively, in T/B cells; (2) in cancer cell lines, the contribution of both carrier systems to *anti*-¹⁴C]FACBC transport was 50:50 and this ratio is pH-dependent; and (3) Na⁺-independent AATs (especially system L) were predominant in [¹⁴C]Met uptake in cancer cells.

Generally, AA PET tracers such as [¹¹C]Met, *O*-¹⁸F-fluoroethyl-L-tyrosine, and *O*-¹⁸F-fluoromethyl-L-tyrosine are thought to be preferable for the differentiation of tumor and inflammatory tissues, because they are taken up substantially by cancer cells but not inflammatory cells in comparison to [¹⁸F]FDG [14, 15]. We previously showed an apparently higher ratio of tumor-to-inflammation accumulation for *anti*-¹⁸F]FACBC than [¹⁸F]FDG using a rat PCa and lymphadenitis model *in vivo* [5]. However, recent pre-clinical and clinical studies revealed [¹¹C]Met uptake in inflamed regions [15, 16]. Moreover, some false-positive uptake, possibly by the accumulation of *anti*-¹⁸F]FACBC in inflammatory regions such as prostatitis and benign prostatic hyperplasia, has been reported in PCa patients [7]. In fact, we show relatively low tumor-to-inflammatory cell *anti*-¹⁴C]FACBC uptake ratios (especially against activated T/B cells), though much higher tumor-to-inflammatory cell uptake ratios were observed with macrophages and granulocytes.

Anti-tumor responses by inflammatory cells and tumor-promoting inflammation coexist in the tumor microenvironment, and an inflammatory microenvironment is essential for all tumors [17]. Inflammatory cells in the tumor microenvironment serve as sources of cytokines and chemokines, which are essential for establishing cancer implant viability [17]. It is estimated that 80 % of PCa patients have some degree of inflammation in the prostate [8]. Although several kinds of inflammatory cells such as T/B cells, neutrophils, macrophages, dendritic cells, and mast cells are observed in the tumor microenvironment [17], lymphocytes are most frequently observed in PCa, and macrophages and neutrophils to a lesser extent [8]. These inflammatory cells are detected even in normal prostate and benign prostatic hyperplasia; 70–80 % as T cells and 10–15 % as B cells, with approximately 40 % of the intra-prostatic T cells activated [8].

AAT expression in inflammatory cells has been reported. For example, T and/or B cells show cell-surface expression of systems ASC (ASCT1, ASCT2), L (LAT1), and A (SNAT1, SNAT2), but not X_C⁻ (xCT) [18–21]; these levels increase on activation [22–24]. Among these, systems A, ASC, and L are the main neutral AA transport systems in mammalian cells, and are over-expressed in various cancers including PCa [25]. Consequently, the transport routes of naturally occurring AAs in activated inflammatory cells and cancerous cells are thought to be similar. As discussed above, systems ASC and L would be the main carriers for *anti*-¹⁸F]FACBC transport in activated T cells and cancer cells, although their contributions would vary somewhat with

extracellular pH changes. Moreover, we have reported that *anti*-[¹⁴C]FACBC uptake into cells is likely similar to that of L-glutamine, because L-glutamine is the most effective *anti*-[¹⁴C]FACBC uptake inhibitor in the presence of Na⁺, and the affinities (K_m) of *anti*-[¹⁴C]FACBC and L-glutamine for ASCT2 were similar (92 and 24–90 μM, respectively) [10, 11]. L-Glutamine is the most abundant AA in blood and is thought to be as important as glucose as fuel for cancer cells as well as inflammatory cells; it is essential for inflammatory cell functions such as T cell proliferation, B cell differentiation, macrophage phagocytosis and antigen-presentation, and neutrophil superoxide production [26]. We therefore concluded that the relatively high *anti*-[¹⁸F]FACBC accumulation in tumor cells and in T/B cells is caused by its preference for system ASC, and some false-positives caused by *anti*-[¹⁸F]FACBC accumulation in inflamed regions are inevitable in FACBC-PET of prostate and other cancer patients [7].

Recently, glutamine-based PET tracers such as L-[5-¹¹C]-glutamine and ¹⁸F-(2S,4R)-4-fluoroglutamine have been reported to clearly visualize glioma and mammary tumors in rodent models [27, 28]. Because the uptake mechanisms of these tracers are likely to be more specific for ASCT2 than that of *anti*-[¹⁸F]FACBC, the process of glutamine-based tracer uptake by inflammatory cells would be interesting.

FDG-PET may exhibit false-positive uptake caused by [¹⁸F]FDG accumulation at lesions such as abscesses and granulomatous areas, including activated inflammatory cells in cancer patients [29]. For example, glioma patients exhibit significant neutrophil infiltration, the degree of which correlated well with the tumor malignancy grade [30]. Kaim et al. [31] showed that several neutrophils infiltrated into abscesses containing central necrosis, and the increased [¹⁸F]FDG accumulation corresponded to granulocyte infiltration in a rat abscess model. Furthermore, [¹¹C]Met, but not [¹⁸F]FDG, has been shown to be useful for differentiating cancerous lesions from granulomatous reactions [32] or radiation necrosis after radiotherapy for glioma [33]. Here, *anti*-[¹⁴C]FACBC and [¹⁴C]Met uptake was relatively high in activated T and/or B cells, but low in activated granulocytes and macrophages compared to tumor cells. Taken together, FACBC-PET may have a lower false-positive uptake than FDG-PET by improving tumor delineation in patients with acutely inflamed lesions, though it may be disadvantageous with chronic inflammation.

Using rat inflammatory cells, we have demonstrated the possibility that *anti*-[¹⁸F]FACBC accumulates in inflammation, especially in activated T/B cells, to a greater extent than previously believed. However, species differences between humans and rodents have been disputed in pharmacokinetics. In fact, it has been reported that some AATs, such as LAT1 and ASCT2, show lower expression at the blood–brain barrier in humans than in mice [34]. Species differences in AAT expression between human and rat inflammatory cells might exist; thus, we recognize the critical importance of *anti*-[¹⁸F]FACBC transport studies in human inflammatory cells. Moreover, further investigation of more complex *in vivo* conditions and in the tumor microenvironment is

warranted to understand the possibility of false-positive uptake and the usefulness of *anti*-[¹⁸F]FACBC imaging for cancer patients.

Conclusion

Our study suggests that significant uptake of *anti*-[¹⁸F]FACBC into activated T/B cells is inevitable and might cause false-positives in FACBC-PET imaging of cancer patients. However, *anti*-[¹⁸F]FACBC is expected to have less false-positives compared with FDG-PET, because of its low uptake into granulocytes and macrophages. Furthermore, the central player for *anti*-[¹⁸F]FACBC transport in T/B cells is system ASC, while that for [¹¹C]Met is system L. Both systems are important for *anti*-[¹⁸F]FACBC uptake in tumor cells, but system L is responsible for [¹¹C]Met uptake. Therefore, the relatively high *anti*-[¹⁸F]FACBC accumulation not only in tumor cells but also in T/B cells is likely caused by its preference for system ASC.

Acknowledgments. The authors thank Mr. Shiro Yoshida and Ms. Sachiko Naito for their assistance in animal treatments and cell cultures, respectively.

Conflict of interest. Shuntaro Oka, Hiroyuki Okudaira, Masahiro Ono, and Yoshifumi Shirakami are employees of Nihon Medi-Physics Co. Ltd. Mark M. Goodman and Emory University have patent rights for *anti*-[¹⁸F]FACBC and are eligible to receive royalties on *anti*-[¹⁸F]FACBC from Nihon Medi-Physics Co. Ltd. Mark M. Goodman, David M. Schuster, and Keiichi Kawai have ongoing research collaborations with Nihon Medi-Physics Co. Ltd.

References

- Fanti S, Franchi R, Battista G et al (2005) PET and PET-CT. State of the art and future prospects. *Radiol Med* 110:1–15
- Singhal T, Narayanan TK, Jain V et al (2008) ¹¹C-L-methionine positron emission tomography in the clinical management of cerebral gliomas. *Mol Imaging Biol* 10:1–18
- Shoup TM, Olson J, Hoffman JM et al (1999) Synthesis and evaluation of [¹⁸F]-1-amino-3-fluorocyclobutane-1-carboxylic acid to image brain tumors. *J Nucl Med* 40:331–338
- Akhurst T, Beattie B, Gogiberidze G, et al. (2006) [¹⁸F]FACBC imaging of recurrent gliomas: a comparison with [¹¹C]methionine and MRI [abstract]. *J Nucl Med* 47:79P.
- Oka S, Hattori R, Kurosaki F et al (2007) A preliminary study of *anti*-1-amino-3-¹⁸F-fluorocyclobutyl-1-carboxylic acid for the detection of prostate cancer. *J Nucl Med* 48:46–55
- Sasajima T, Ono T, Shimada N et al (2013) *Trans*-1-amino-3-¹⁸F-fluorocyclobutanecarboxylic acid (*anti*-¹⁸F-FACBC) is a feasible alternative to ¹¹C-methyl-L-methionine and magnetic resonance imaging for monitoring treatment response in gliomas. *Nucl Med Biol* 40:808–815
- Schuster DM, Taleghani PA, Nieh PT et al (2013) Characterization of primary prostate carcinoma by *anti*-1-amino-2-[¹⁸F]-fluorocyclobutane-1-carboxylic acid (*anti*-3-[¹⁸F] FACBC) uptake. *Am J Nucl Med Mol Imaging* 3:85–96
- Sfanos KS, De Marzo AM (2012) Prostate cancer and inflammation: the evidence. *Histopathology* 60:199–215
- Okudaira H, Shikano N, Nishii R et al (2011) Putative transport mechanism and intracellular fate of *trans*-1-amino-3-¹⁸F-fluorocyclobutanecarboxylic acid in human prostate cancer. *J Nucl Med* 52:822–829
- Oka S, Okudaira H, Yoshida Y et al (2012) Transport mechanisms of *trans*-1-amino-3-fluoro[1-¹⁴C]cyclobutanecarboxylic acid in prostate cancer cells. *Nucl Med Biol* 39:109–119
- Okudaira H, Nakanishi T, Oka S et al (2013) Kinetic analyses of *trans*-1-amino-3-[¹⁸F]fluorocyclobutanecarboxylic acid transport in *Xenopus laevis* oocytes expressing human ASCT2 and SNAT2. *Nucl Med Biol* 40:670–675

12. Hediger MA, Romero MF, Peng JB et al (2004) The ABCs of solute carriers: physiological, pathological and therapeutic implications of human membrane transport proteins. *Pflugers Arch* 447:465–468
13. Kanai Y, Fukasawa Y, Cha SH et al (2000) Transport properties of a system y^L neutral and basic AA transporter. Insights into the mechanisms of substrate recognition. *J Biol Chem* 275:20787–20793
14. Rau FC, Weber WA, Wester HJ et al (2002) *O*-(2-[¹⁸F]Fluoroethyl)-L-tyrosine (FET): a tracer for differentiation of tumour from inflammation in murine lymph nodes. *Eur J Nucl Med Mol Imaging* 29:1039–1046
15. Tsukada H, Sato K, Fukumoto D et al (2006) Evaluation of D-isomers of *O*-¹¹C-methyl tyrosine and *O*-¹⁸F-fluoromethyl tyrosine as tumor-imaging agents in tumor-bearing mice: comparison with L- and D-¹¹C-methionine. *J Nucl Med* 47:679–688
16. Tsuyuguchi N, Sunada I, Ohata K et al (2003) Evaluation of treatment effects in brain abscess with positron emission tomography: comparison of fluorine-18-fluorodeoxyglucose and carbon-11-methionine. *Ann Nucl Med* 17:47–51
17. Grivennikov SI, Greten FR, Karin M (2010) Immunity, inflammation, and cancer. *Cell* 140:883–899
18. Segel GB, Simon W, Lichtman MA (1984) Multicomponent analysis of amino acid transport in human lymphocytes. Diminished L-system transport in chronic leukemic B lymphocytes. *J Clin Invest* 74:17–24
19. Ishii T, Sugita Y, Bannai S (1987) Regulation of glutathione levels in mouse spleen lymphocytes by transport of cysteine. *J Cell Physiol* 133:330–336
20. Gmünder H, Eck HP, Dröge W (1991) Low membrane transport activity for cystine in resting and mitogenically stimulated human lymphocyte preparations and human T cell clones. *Eur J Biochem* 201:113–117
21. Iruloh CG, D'Souza SW, Fergusson WD et al (2009) Amino acid transport systems beta and A in fetal T lymphocytes in intrauterine growth restriction and with tumor necrosis factor-alpha treatment. *Pediatr Res* 65:51–56
22. Gaugitsch HW, Prieschl EE, Kalthoff F et al (1992) A novel transiently expressed, integral membrane protein linked to cell activation. Molecular cloning via the rapid degradation signal AUUUA. *J Biol Chem* 267:11267–11273
23. Matsumoto Y, Satoh-Ueno K, Yoshimura A et al (1999) Identification and immunological characterization of a novel 40-kDa protein linked to CD98 antigen. *Cell Struct Funct* 24:217–226
24. Levring TB, Hansen AK, Nielsen BL et al (2012) Activated human CD4⁺ T cells express transporters for both cysteine and cystine. *Sci Rep* 2:266
25. Fuchs BC, Bode BP (2005) Amino acid transporters ASCT2 and LAT1 in cancer: partners in crime? *Semin Cancer Biol* 15:254–266
26. Newsholme P (2001) Why is L-glutamine metabolism important to cells of the immune system in health, postinjury, surgery or infection? *J Nutr* 131:2515S–2522S
27. Qu W, Oya S, Lieberman BP et al (2012) Preparation and characterization of L-[5-¹¹C]-glutamine for metabolic imaging of tumors. *J Nucl Med* 53:98–105
28. Ploessl K, Wang L, Lieberman BP et al (2012) Comparative evaluation of ¹⁸F-labeled glutamic acid and glutamine as tumor metabolic imaging agents. *J Nucl Med* 53:1616–1624
29. Shreve PD, Anzai Y, Wahl RL (1999) Pitfalls in oncologic diagnosis with FDG PET imaging: physiologic and benign variants. *Radiographics* 19:61–77
30. Fossati G, Ricevuti G, Edwards SW et al (1999) Neutrophil infiltration into human gliomas. *Acta Neuropathol* 98:349–354
31. Kaim AH, Weber B, Kurrer MO et al (2002) Autoradiographic quantification of ¹⁸F-FDG uptake in experimental soft-tissue abscesses in rats. *Radiology* 223:446–451
32. Zhao S, Kuge Y, Kohanawa M et al (2008) Usefulness of ¹¹C-methionine for differentiating tumors from granulomas in experimental rat models: a comparison with ¹⁸F-FDG and ¹⁸F-FLT. *J Nucl Med* 49:135–141
33. Terakawa Y, Tsuyuguchi N, Iwai Y et al (2008) Diagnostic accuracy of ¹¹C-methionine PET for differentiation of recurrent brain tumors from radiation necrosis after radiotherapy. *J Nucl Med* 49:694–699
34. Ohtsuki S, Uchida Y, Kubo Y, Terasaki T (2011) Quantitative targeted absolute proteomics-based ADME research as a new path to drug discovery and development: methodology, advantages, strategy, and prospects. *J Pharm Sci* 100:3547–3559